Full Temporal Characterization of Ultrabroadband Few-Cycle Laser Pulses Using Atomically Thin WS$_2$

Hernandez-Rueda, Javier; Pérez-Benito, Óscar; Martínez Maestro, Laura; Noordam, Marc L.; Kuipers, L.; Weigand, Rosa

Important note
To cite this publication, please use the final published version (if applicable).
Please check the document version above.

Article

Full Temporal Characterization of Ultrabroadband Few-Cycle Laser Pulses Using Atomically Thin WS$_2$

Óscar Pérez-Benito, Javier Hernandez-Rueda,* Laura Martínez Maestro, Marc L. Noordam, L. Kuipers, and Rosa Weigand

Cite This: https://doi.org/10.1021/acsphotonics.3c00353

Read Online

ACCESS | Metrics & More | Article Recommendations | Supporting Information

ABSTRACT: Nowadays, the accurate and full temporal characterization of ultrabroadband few-cycle laser pulses with pulse durations below 7 fs is of great importance in fields of science that investigate ultrafast dynamic processes. There are several indirect methods that use nonlinear optical signals to retrieve the complex electric field of femtosecond lasers. However, the precise characterization of few-cycle femtosecond laser sources with an ultrabroadband spectrum presents additional difficulties, such as reabsorption of nonlinear signals, partial phase matching, and spatiotemporal mismatches. In this work, we combine the dispersion scan (d-scan) method with atomically thin WS$_2$ flakes to overcome these difficulties and fully characterize ultrabroadband laser pulses with a pulse duration of 6.9 fs and a spectrum that ranges from 650 to 1050 nm. Two-dimensional WS$_2$ acts as a remarkably efficient nonlinear medium that offers a broad transparency range and allows for achieving relaxed phase-matching conditions due to its atomic thickness. Using mono- and trilayers of WS$_2$, we acquire d-scan traces by measuring the second-harmonic generation (SHG) signal, originated via laser—WS$_2$ interaction, as a function of optical dispersion (i.e., glass thickness) and wavelength. Our retrieval algorithm extracts a pulse duration at full-width half-maximum of 6.9 fs and the same spectral phase function irrespective of the number of layers. We benchmark and validate our results obtained using WS$_2$ by comparing them with those obtained using a 10-μm-thick BBO crystal. Our findings show that atomically thin media can be an interesting alternative to micrometer-thick bulk crystals to characterize ultrabroadband femtosecond laser pulses using SHG-d-scan with an error below 100 as (attoseconds).

KEYWORDS: Ultrabroadband femtosecond lasers, d-scan, 2D materials, transition metal dichalcogenides, second-harmonic generation, nonlinear optics, WS$_2$
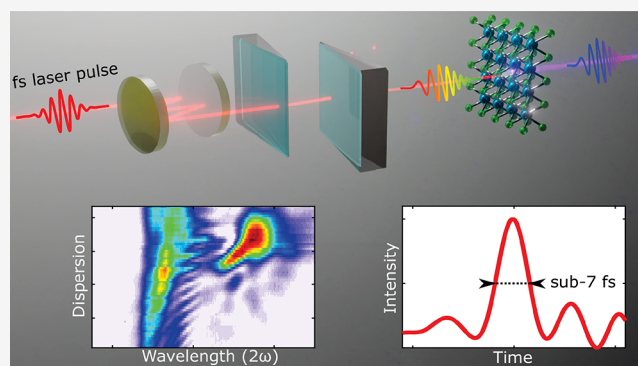
INTRODUCTION

The full temporal characterization of ultrabroadband few-cycle laser pulses is highly relevant in the fields of nanophotonics,[1−3] biology,[4] nonlinear optics,[5,6] and attosecond science[7−9] in order to investigate ultrafast dynamic processes. Few-cycle Ti:sapphire (Ti:Sa) lasers typically deliver pulses with durations below 10 fs and highly structured spectra of a few hundreds of nanometers bandwidth. Their unique features make them specially useful to enhance the performance of techniques such as ultrafast spectroscopy[10−12] or time-resolved microscopy[3,13] by simultaneously providing an unprecedented temporal resolution and a broad spectral bandwidth. Over the past decades, the scientific community has developed several techniques to characterize lasers with femtosecond pulse durations, such as frequency-resolved optical gating (FROG),[14−16] spectral-phase interferometry for direct electric-field reconstruction (SPIDER),[17] multiphoton intrapulse interference phase scan (MIIPS),[18] dispersion scan (d-

scan),[19,20] and amplitude swing.[21] However, the full temporal characterization of few-cycle lasers is particularly challenging compared to measuring their temporally longer and spectrally narrower counterparts. On one hand, the intensity profile of few-cycle laser pulses changes almost as fast as their electric field oscillates. On the other hand, they typically possess highly complex, structured, and broad spectra.

In contrast with other methods, the inline geometry used by d-scan makes it an advantageous technique to characterize ultrabroadband few-cycle laser pulses, as it avoids issues related to aligning multiple laser beams or dealing with a limited
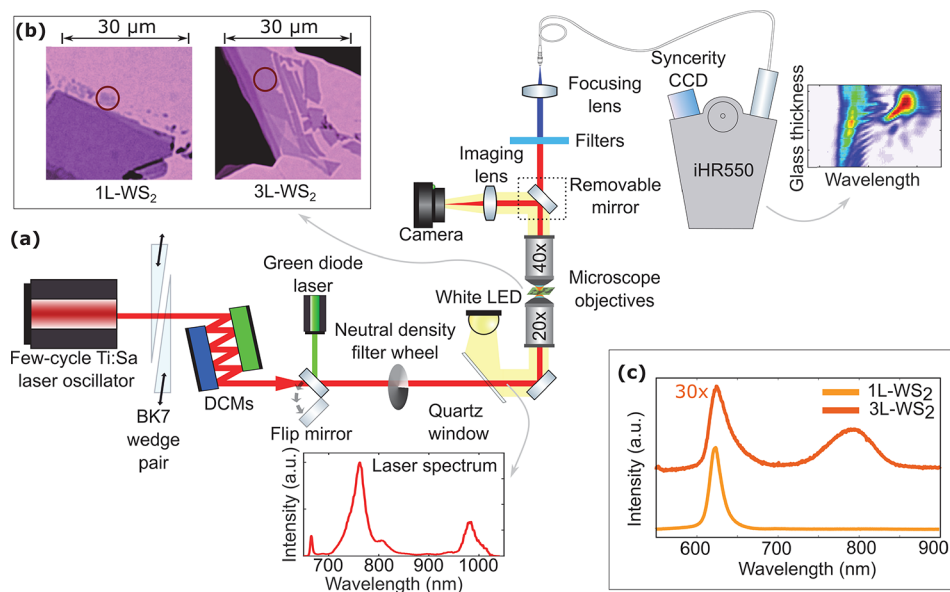
Figure 1. (a) Schematic of our d-scan experimental setup. The femtosecond-laser oscillator delivers ultrabroadband light pulses that pass through two opposed BK7 wedges and DCM mirrors, which introduce optical dispersion. The beam is then focused using a microscope objective on the nonlinear medium (i.e., WS_2 or BBO) producing SHG. This signal is collected with a second objective and sent to the spectrometer. The insets present the laser spectrum measured right before entering the microscope and a typical d-scan trace (i.e., SHG intensity as a function of glass thickness and wavelength). (b) Optical microscopy images of WS_2 flakes. The marked regions illustrate the precise locations used in the experiments. (c) PL spectra of the regions marked in panel b.

temporal resolution when using optical delay lines (i.e., limited step size in motors). The d-scan method uses nonlinear optical signals that result from the interaction of a single laser beam (i.e., inline geometry) with a thin nonlinear medium while introducing a controlled amount of optical dispersion.[19,20] Second-harmonic generation (SHG) is the most common nonlinear signal used in this method, although other nonlinear signals have also been explored.[22,23] The dispersion experienced by the laser pulses is carefully controlled by varying the insertion of a pair of glass wedges (i.e., the glass thickness traversed by the pulse) and the number of bounces on chirped mirror pairs. Therefore, d-scan measurements register the intensity of a certain nonlinear optical signal as a function of wavelength and optical dispersion, i.e., d-scan traces, from which the full information on the electric field of the laser pulse can be retrieved. To that end, simulated traces are generated using an iterative retrieval routine that uses (a) an algorithm to emulate the specific nonlinear optical process at play and (b) specific optimization schemes that minimize the difference between experimental and simulated traces.[19,20,22−26]

d-scan systems usually employ very thin nonlinear crystals (around 10−20 μm), such as β-barium borate crystals (BBO). Nonlinear media based on nanosystems, like ensembles of dielectric nanoparticles, have also been used in order to achieve relaxed phase-matching conditions for a wide spectral bandwidth.[20] However, nanosized media can only be used at the expense of adding an additional incoherent term to retrieval algorithms, which represents the scattering of laser light by nanoparticles.[20] The use of two-dimensional (2D) materials poses an interesting alternative as their unique optical properties[27] can help to simultaneously overcome several limitations intrinsic to other nonlinear media or temporal characterization methods. Their atomically thin nature allows for achieving relaxed phase-matching conditions while presenting an extremely high nonlinear optical response.[28] For example third-harmonic generation (THG) generated in

graphene has been used to characterize few-cycle laser pulses in the near- to mid-infrared using d-scan.[29] However, larger nonlinear optical signals can be obtained from second-order processes in noncentrosymmetric 2D materials, such as SHG in TMDCs. Such processes lead to a higher conversion efficiency compared to their higher order counterparts (i.e., THG in graphene) and consequently require a lower laser intensity to generate light; thus, these are less susceptible to damage the nonlinear 2D medium. Several degenerate and nondegenerate second-order nonlinear mechanisms have been studied in a variety of 2D materials[30−37] and exploited in FROG systems to characterize laser pulses with pulse durations above 100 fs and bandwidths of ~10 nm.[38,39] In addition, 2D-layered transition metal dichalcogenides (TMDCs) present a broad spectral range of transparency,[40,41] which can help to minimize reabsorption of the nonlinearly generated signals. Therefore, these materials offer an attractive alternative for spectral regions in which nonlinear crystals may not be available. From a technical point of view, 2D TMDCs offer a relatively high damage threshold[42] and their exfoliation-based fabrication is relatively inexpensive when compared to the cost of ultrathin nonlinear crystals or nanostructured metallic materials used for laser pulse characterization in d-scan and FROG systems. In contrast, ultrathin nonlinear crystals achieve a superior conversion efficiency of nonlinearly generated signals due to their dramatically longer interaction length. In addition to these advantageous features, the number of atomic layers in 2D TMDC samples can be readily characterized by measuring their photoluminescence (PL) spectral signature when excited using a low-power continuous-wave (cw) laser.[43−45]

In this paper, we combine the SHG-based d-scan method with atomically thin flakes of WS_2 in order to fully characterize ultrabroadband few-cycle femtosecond-laser pulses (see Figure 1a). We make use of atomically thin WS_2 flakes to take advantage of their remarkably high nonlinear second-order

susceptibility and transparency over a broad spectral range. Besides, their atomically thin nature allows for achieving relaxed phase-matching conditions. We measure d-scan traces using mono- and trilayers of WS_2 and find excellent agreement among the retrieved temporal intensity distributions. We validate the results extracted from traces measured with WS_2 by comparing them with those obtained using a BBO crystal, illustrating that WS_2, and TMDCs by extension, can be used as new nonlinear media in d-scan systems. The full temporal information on our laser field is extracted from the experimental traces using a retrieval algorithm which is well established in the literature.[46] Furthermore, using our method, we are able to systematically characterize the laser pulse duration with an error below 100 as (attoseconds).

■ METHODS

The nonlinear media employed in the experiments consist of WS_2 flakes exfoliated on a thin glass slide and a 10-μm-thick commercial BBO crystal. We carry out the WS_2 sample preparation in a cleanroom environment where bulk WS_2 is mechanically exfoliated and deposited onto a glass slide using the adhesive tape technique.[44] Prior to transferring the WS_2 flakes, we clean the glass substrate using diluted acid solutions and an oxygen plasma cleaner. We use a home-built optical microscope, described in Figure 1a, to locate flakes of interest that contain thin layers of WS_2 (see Figure 1b) and subsequently measure their PL signal to identify their thickness (Figure 1c). The sample can be illuminated using light generated by either a white LED or a cw diode laser at 532 nm, which is introduced by a quartz window or a flip mirror, respectively. The white LED serves as the illumination source for the in situ visualization system (removable mirror, imaging lens, and CCD camera) that is used to inspect the sample surface, locate flakes, and aim the lasers at the desired spot. Using the green laser, we measure the PL emissions shown in Figure 1c that we use to characterize the WS_2 layer thickness. Figure 1c presents the PL spectra of the marked areas of the WS_2 flakes shown in Figure 1b with 1 (orange) and 3 (brown) atomic layers. The spectrum of the monolayer illustrates a sole peak centered around 625 nm, which corresponds to the A exciton.[43] The spectrum of the trilayer also illustrates the A exciton peak and presents an additional peak centered at 800 nm that corresponds to the indirect band-gap emission. More details of the relationship between the PL spectral signature of WS_2 and the number of atomic layers can be found in Zeng et al.[43] and Gong et al.[44]

For the laser–WS_2 interaction experiments, we use the experimental setup shown in Figure 1a. We employ a home-built Ti:Sa oscillator that delivers horizontally polarized few-cycle femtosecond-laser pulses with a pulse duration of ~6.9 fs and a spectral range from 650 to 1050 nm at a repetition rate of 78 MHz. The laser operates in TEM_{00} mode with a beam diameter of 840 μm at full-width half-maximum (fwhm).[47] The d-scan setup combines an optical compression unit, a microscope, and a spectrometer.

First, the laser passes through the compression unit, a dispersion-control system, which uses a BK7 wedge pair (8°) mounted on two opposed motorized translation stages and two rectangular chirped mirror pairs (DCM7 from Venteon, 19 bounce pairs in total). These elements introduce a controlled amount of optical dispersion by modifying the glass thickness z through the insertion of the wedges while keeping a constant number of bounces for the mirrors. As a result, an additional

spectral phase $\varphi(\omega, z)$ is added to the laser field. We use a reflective neutral density gradient filter wheel to attenuate the laser average power down to 3 mW, which is well below the damage threshold (~20 mW for WS_2 under our focusing conditions). We neglect a significant inhomogeneity imprinted on the laser spatial distribution due to (a) the reduced millimeter size of the beam and (b) aligning the beam at the edge of the filter wheel. Afterward, the laser beam is steered toward a home-built microscope and is focused onto the WS_2 sample using a microscope objective (Olympus Plan N, 20×, NA = 0.40, USI2), resulting in a SHG signal centered around 385 nm. The frequency-doubled signal is collected by a second objective (Olympus LUCPlanFL N, 40×, NA = 0.6, FN22), filtered (2× Schott BG40 and Schott BG23 filters), and focused (UV fused silica lens, f = 5 cm) onto an optical fiber head (Thorlabs, M114L02, solarized, core size 600 μm, NA = 0.22) that guides the light toward a spectrometer (Horiba iHR550 equipped with a low-noise cooled camera, model Syncerity). We checked that the intensity of the SHG signal (I_{SHG}) depends on the second power of the input laser intensity I following the law $I_{SHG} \propto I^2$. Note that the green laser and the femtosecond laser are spatially overlapped, and thus, both the PL spectra and the d-scan traces were measured at the exact same location. The experimental data acquisition routine is typically limited to a time span of a few hours in which the stability of the laser is periodically monitored by recording the laser spectrum. d-scan data acquired using WS_2 and BBO media are always measured during the same experimental run. This procedure avoids issues related to potential instabilities and minute temporal variations of the femtosecond-laser oscillator.

Using the experimental setup, we measure both the fundamental laser spectrum $I(\omega)$ at the entrance of the microscope and d-scan traces, which are fed to our algorithm allowing us to retrieve the spectral phase $\phi(\omega)$ of the laser.[19,20,25] The inset of Figure 1a depicts an example of a typical d-scan trace. The experimental traces S_{exp} consist of false-color maps of the SHG intensity as a function of wavelength and glass thickness z (i.e., optical dispersion). In general, $z = 0$ is assigned to the maximum compression point, where the laser pulse is closest to be Fourier transform-limited. The glass thickness axis is set with respect to this $z = 0$ value, and hence, the axis range may take negative values. The simulated trace S_{sim} can be expressed as

$$S_{sim}(\omega, z) = \mu(\omega) \left| \int_{-\infty}^{+\infty} \left(\int_{-\infty}^{+\infty} \tilde{E}(\Omega) e^{-ik(\Omega)z} e^{i\Omega t} \, d\Omega \right)^2 e^{-i\omega t} \, dt \right|^2$$

(1)

where $\tilde{E}(\omega) = \sqrt{I(\omega)} \, e^{i\phi(\omega)}$ stands for the complex electric field of the laser pulse in the spectral domain and $\varphi(\omega, z) = k(\omega)z$ accounts for the spectral phase introduced by the glass wedges. The function $\mu(\omega)$ contains information on the spectral response of different optical components (lenses, mirrors, etc.) as well as encodes the SHG efficiency curve of the nonlinear material. This function is calculated within the retrieval process. Equation 1 is embedded in a retrieval algorithm, which through an iterative routine proposes different spectral phases $\phi(\omega)$. More details of the d-scan retrieval algorithm, the minimization routine, and the error calculation can be found in the Supporting Information and in Pérez-Benito and Weigand.[20] The criterion to update $\phi(\omega)$ is to minimize an error G, which evaluates the difference between

the simulated and the experimental traces (S_{sim} and S_{exp}, respectively). If the calculated error is below the criterion of $G \leq 0.03$, the retrieval is considered successful, and by applying an inverse Fourier transform to the extracted field in the spectral domain $\tilde{E}(\omega)$, we obtain the electric field in the temporal domain $E(t)$ and the intensity distribution of the laser pulse $I(t)$.

RESULTS

Figure 2 shows SHG d-scan traces measured using a WS$_2$ monolayer (Figure 2a) and a 10-μm-thick BBO crystal (Figure
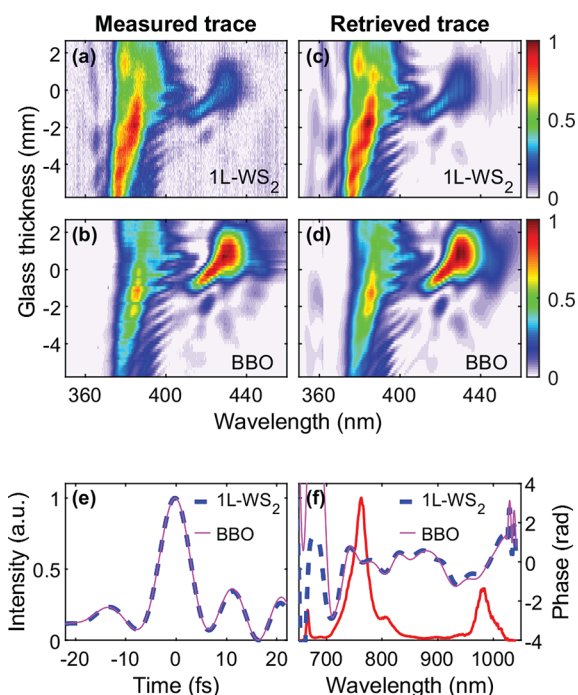

Figure 2. Experimental d-scan traces obtained using (a) a WS$_2$ monolayer and (b) a 10-μm-thick BBO crystal. (c and d) Retrieved traces after applying our spectral-phase-retrieval algorithm to the traces depicted in (a) and (b), respectively. (e) Time−intensity distributions of the laser pulses. (f) Laser spectrum (red) and spectral phases.

2b) in combination with our few-cycle laser oscillator. The experimental traces $S_{\text{exp}}(\omega, z)$ were acquired for a total glass thickness range of $\Delta z = 8$ mm. The SHG spectra were measured from 350 to 450 nm and are sensitive to the spectral phase. Qualitatively, the experimental traces present a similar shape for both nonlinear media, although WS$_2$ illustrates a higher relative SHG efficiency for shorter wavelengths than BBO, evidencing the different spectral response of these media. Figure 2c and 2d corresponds to the retrieved traces $S_{\text{sim}}(\omega, z)$. These traces are obtained by our algorithm and allow us to extract the electric field of the laser $\tilde{E}(\omega)$, as detailed in the Methods section. We reiterate that our algorithm only requires one to use a coherent field to describe the laser−WS$_2$ interaction. This renders our WS$_2$-based d-scan as an alternative method that does not need to take into account incoherent fields within the algorithm, as it is required when using clusters of dielectric nanoparticles.[20] This is due to the fact that the area of the flakes is large enough to avoid border effects that potentially give rise to scattering. The average errors found for the WS$_2$ and BBO trace retrievals are $G =$

0.025 and 0.021, respectively. From this point forth, we present the results of the retrievals in Table 1 in order to facilitate a

Table 1. Results Obtained Using WS$_2$ or BBO

medium	thickness	pulse duration (fs)	error G
BBO	10 μm	6.9 ± 0.1	0.021
WS$_2$	monolayer	6.9 ± 0.1	0.025
WS$_2$	trilayer	6.9 ± 0.1	0.023

direct comparison among results attained using different nonlinear media. Each pulse duration presented in Table 1 is the average of the pulse durations obtained from 10 independent retrievals of its corresponding d-scan trace, while the errors have been estimated by calculating the standard deviation of those pulse durations. Figure 2e illustrates a good correspondence for the retrieved temporal intensity distributions, which both lead to a pulse duration at fwhm of 6.9 ± 0.1 fs. Figure 2f shows the laser spectrum and the retrieved spectral phase, which also evidence a good agreement between the results extracted from both d-scan traces. The relative errors between the pulse profiles obtained using WS$_2$ flakes and BBO are below 5%. We calculate these using the expression $|I_{\text{WS}_2}(t) - I_{\text{BBO}}(t)|/I_{\text{BBO}}(t)$ in a time range equivalent to four times the retrieved pulse duration. Here, we provide evidence that results independently obtained using a WS$_2$ monolayer and a thin BBO crystal show excellent agreement, which serves to benchmark the validity of using atomically thin WS$_2$ flakes as nonlinear media.

In Figure 3a and 3b, we present d-scan traces obtained using WS$_2$ flakes with one (Figure 3a) and three (Figure 3b) atomic layers. Qualitatively, the traces show the same appearance
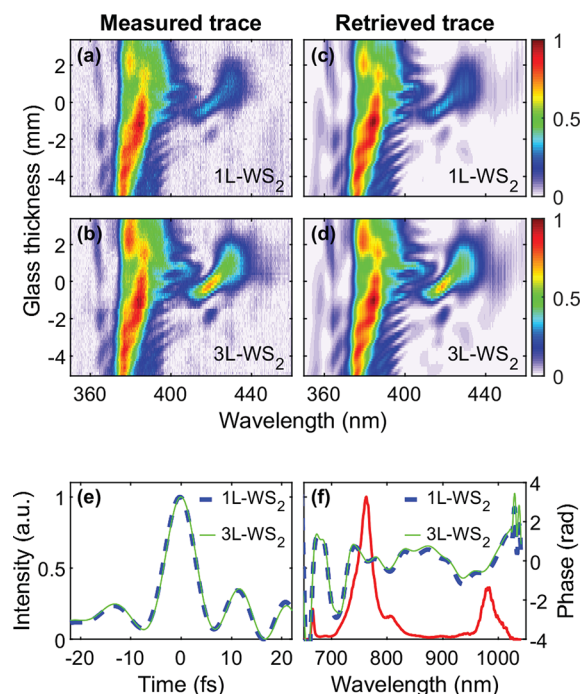

Figure 3. (a and b) Experimental d-scan traces obtained using a monolayer (top) and trilayer (middle) of WS$_2$. (c and d) Retrieved d-scan traces of the experiments shown in the right column. (e) Time−intensity distributions of the laser pulses. (f) Laser spectrum (red) and spectral phases.

irrespective of the number of atomic layers. Quantitatively, we observed a higher SHG signal for WS_2 monolayers. It is worth noticing that under the same experimental conditions, we did not observe a measurable SHG signal originated at the glass substrate nor for flakes with an even number of layers, as these flakes are centrosymmetric.[32] Besides, bulky and thicker (>5 atomic layers) WS_2 flakes yield a dim SHG signal that is almost entirely reabsorbed when performing measurements in transmission mode. We reiterate that the traces were measured at the precise locations where the PL measurements were done as shown in Figure 1b. The left and right panels again depict experimental and retrieved traces, respectively. The errors of the trace retrieval in Figure 3c and 3d are both close to $G = 0.025$. We find good agreement among results consisting of the retrieved temporal intensity distribution or spectral phase extracted from traces measured for different layer number, as shown in Figure 3e and 3f. We consistently find a pulse duration (fwhm) of 6.9 ± 0.1 fs for the regions of WS_2 with 1 and 3 atomic layers, as summarized in Table 1. These findings are in line with the pulse duration retrieved from traces measured using a BBO crystal as discussed in Figure 2. In addition to the measurements shown in Figure 3, we also performed a set of measurements of laser pulses with a pulse duration of 12 fs by setting the spectrum of the laser oscillator to be narrower (see Supporting Information), illustrating the validity of our method for other experimental conditions. Our results provide evidence of the high accuracy and reproducibility of using atomically thin WS_2 within a d-scan setup with the purpose of characterizing few-cycle Ti:Sa laser pulses. We note here that the use of chemical vapor deposition allows one to fabricate flakes with a larger area than those produced by the exfoliation method, thus facilitating the spatial overlap between the laser beam and the TMDC flakes. Other atomically thin TMDCs have potential to be exploited as alternative nonlinear media for ultrabroadband few-cycle laser pulse characterization in other spectral ranges, which can be achieved by carefully selecting a TMDC whose excitonic emission does not overlap with the SHG signal.

CONCLUSIONS

We have used atomically thin WS_2 flakes combined with d-scan to fully characterize ultrabroadband few-cycle femtosecond-laser pulses from a Ti:Sa oscillator in the VIS−IR range with a pulse duration of 6.9 fs. Atomically thin flakes of WS_2 favor the characterization of laser pulses with a few optical cycles over other nonlinear media as they simultaneously (i) exhibit an extraordinarily high nonlinear optical response, (ii) exhibit a broad spectral range of transparency, and (iii) allow for achieving relaxed phase-matching conditions. WS_2 monolayers provide a higher SHG efficiency and a larger transmission coefficient compared to their thicker counterparts, easing the acquisition of d-scan traces. The absence of scattering within 2D flakes of WS_2 allows us to consider only the same physical processes (SHG) and retrieval techniques used for bulk crystals without the need to consider additional physical processes to describe the laser−layers interaction, such as scattering. This aids one to retrieve pulse durations with a temporal accuracy on the order of 100 as. This work opens up a new venue to employ other 2D semiconductor materials to characterize few-cycle femtosecond-laser pulses with ultra-broadband spectra in different spectral regions.

ASSOCIATED CONTENT

Ⓢ Supporting Information

The Supporting Information is available free of charge at https://pubs.acs.org/doi/10.1021/acsphotonics.3c00353.

Extended details of the d-scan retrieval procedure and additional WS_2-based d-scan experiments using laser pulses with a duration of 12 fs (PDF)

AUTHOR INFORMATION

Corresponding Author

Javier Hernandez-Rueda − *Department of Optics, Faculty of Physics, University Complutense of Madrid, 28040 Madrid, Spain;* ⓘ orcid.org/0000-0002-8723-4832; Email: fj.hernandez.rueda@ucm.es

Authors

Óscar Pérez-Benito − *Department of Optics, Faculty of Physics, University Complutense of Madrid, 28040 Madrid, Spain;* ⓘ orcid.org/0000-0002-3903-5732

Laura Martínez Maestro − *Department of Optics, Faculty of Physics, University Complutense of Madrid, 28040 Madrid, Spain*

Marc L. Noordam − *Kavli Institute of Nanoscience Delft, Department of Quantum Nanoscience, Delft University of Technology, 2628 CJ Delft, The Netherlands;* ⓘ orcid.org/0000-0002-0234-5438

L. Kuipers − *Kavli Institute of Nanoscience Delft, Department of Quantum Nanoscience, Delft University of Technology, 2628 CJ Delft, The Netherlands;* ⓘ orcid.org/0000-0003-0556-8167

Rosa Weigand − *Department of Optics, Faculty of Physics, University Complutense of Madrid, 28040 Madrid, Spain;* ⓘ orcid.org/0000-0003-4045-8043

Complete contact information is available at: https://pubs.acs.org/10.1021/acsphotonics.3c00353

REFERENCES

(1) Ropers, C.; Elsaesser, T.; Cerullo, G.; Zavelani-Rossi, M.; Lienau, C. Ultrafast optical excitations of metallic nanostructures: from light confinement to a novel electron source. *New J. Phys.* **2007**, *9*, 397−397.

(2) Krüger, M.; Lemell, C.; Wachter, G.; Burgdörfer, J.; Hommelhoff, P. Attosecond physics phenomena at nanometric tips. *J. Phys. B: At. Mol. Opt. Phys.* **2018**, *51*, 172001.

(3) Schnedermann, C.; Lim, J. M.; Wende, T.; Duarte, A. S.; Ni, L.; Gu, Q.; Sadhanala, A.; Rao, A.; Kukura, P. Sub-10 fs time-resolved vibronic optical microscopy. *J. Phys. Chem. Lett.* **2016**, *7*, 4854−4859.

(4) Maibohm, C.; Silva, F.; Figueiras, E.; Guerreiro, P. T.; Brito, M.; Romero, R.; Crespo, H.; Nieder, J. B. SyncRGB-FLIM: synchronous fluorescence imaging of red, green and blue dyes enabled by ultra-

broadband few-cycle laser excitation and fluorescence lifetime detection. *Biomed. Opt. Express* **2019**, *10*, 1891−1904.

(5) Johnson, A. S.; Austin, D. R.; Wood, D. A.; Brahms, C.; Gregory, A.; Holzner, K. B.; Jarosch, S.; Larsen, E. W.; Parker, S.; Strüber, C. S.; Ye, P.; Tisch, J. W. G.; Marangos, J. P. High-flux soft x-ray harmonic generation from ionization-shaped few-cycle laser pulses. *Sci. Adv.* **2018**, *4*, eaar3761.

(6) Guan, Z.; Zhou, X.-X.; Bian, X.-B. High-order-harmonic generation from periodic potentials driven by few-cycle laser pulses. *Phys. Rev. A* **2016**, *93*, 033852.

(7) Krausz, F.; Ivanov, M. Attosecond physics. *Rev. Mod. Phys.* **2009**, *81*, 163−234.

(8) Esarey, E.; Schroeder, C.; Leemans, W. Physics of laser-driven plasma-based electron accelerators. *Rev. Mod. Phys.* **2009**, *81*, 1229.

(9) Kärtner, F. X. *Few-cycle laser pulse generation and its applications*; Topics in Applied Physics; Springer: Berlin, Heidelberg, 2004; Vol. 95.

(10) Kowalewski, M.; Fingerhut, B. P.; Dorfman, K. E.; Bennett, K.; Mukamel, S. Simulating coherent multidimensional spectroscopy of nonadiabatic molecular processes: From the infrared to the x-ray regime. *Chem. Rev.* **2017**, *117*, 12165−12226.

(11) Tiwari, V.; Matutes, Y. A.; Gardiner, A. T.; Jansen, T. L.; Cogdell, R. J.; Ogilvie, J. P. Spatially-resolved fluorescence-detected two-dimensional electronic spectroscopy probes varying excitonic structure in photosynthetic bacteria. *Nat. Commun.* **2018**, *9*, 1−10.

(12) Beane, G.; Devkota, T.; Brown, B. S.; Hartland, G. V. Ultrafast measurements of the dynamics of single nanostructures: a review. *Rep. Prog. Phys.* **2019**, *82*, 016401.

(13) Sung, J.; Schnedermann, C.; Ni, L.; Sadhanala, A.; Chen, R.; Cho, C.; Priest, L.; Lim, J. M.; Kim, H.-K.; Monserrat, B.; et al. Long-range ballistic propagation of carriers in methylammonium lead iodide perovskite thin films. *Nat. Phys.* **2020**, *16*, 171−176.

(14) Trebino, R.; DeLong, K. W.; Fittinghoff, D. N.; Sweetser, J. N.; Krumbügel, M. A.; Richman, B. A.; Kane, D. J. Measuring ultrashort laser pulses in the time-frequency domain using frequency-resolved optical gating. *Rev. Sci. Instrum.* **1997**, *68*, 3277−3295.

(15) Baltuška, A.; Pshenichnikov, M. S.; Wiersma, D. A. Amplitude and phase characterization of 4.5-fs pulses by frequency-resolved optical gating. *Opt. Lett.* **1998**, *23*, 1474−1476.

(16) Yang, Z.; Cao, W.; Chen, X.; Zhang, J.; Mo, Y.; Xu, H.; Mi, K.; Zhang, Q.; Lan, P.; Lu, P. All-optical frequency-resolved optical gating for isolated attosecond pulse reconstruction. *Opt. Lett.* **2020**, *45*, 567−570.

(17) Iaconis, C.; Walmsley, I. A. Spectral phase interferometry for direct electric-field reconstruction of ultrashort optical pulses. *Opt. Lett.* **1998**, *23*, 792−794.

(18) Lozovoy, V. V.; Pastirk, I.; Dantus, M. Multiphoton intrapulse interference. IV. Ultrashort laser pulse spectral phase characterization and compensation. *Opt. Lett.* **2004**, *29*, 775−777.

(19) Miranda, M.; Arnold, C. L.; Fordell, T.; Silva, F.; Alonso, B.; Weigand, R.; L'Huillier, A.; Crespo, H. Characterization of broadband few-cycle laser pulses with the d-scan technique. *Opt. Express* **2012**, *20*, 18732−18743.

(20) Pérez-Benito, Ó.; Weigand, R. Nano-dispersion-scan: measurement of sub-7-fs laser pulses using second-harmonic nanoparticles. *Opt. Lett.* **2019**, *44*, 4921−4924.

(21) Alonso, B.; Holgado, W.; Sola, I. J. Compact in-line temporal measurement of laser pulses with amplitude swing. *Opt. Express* **2020**, *28*, 15625−15640.

(22) Canhota, M.; Weigand, R.; Crespo, H. M. Simultaneous measurement of two ultrashort near-ultraviolet pulses produced by a multiplate continuum using dual self-diffraction dispersion-scan. *Opt. Lett.* **2019**, *44*, 1015−1018.

(23) Gomes, T.; Canhota, M.; Crespo, H. Temporal characterization of broadband femtosecond laser pulses by surface third-harmonic dispersion scan with ptychographic retrieval. *Opt. Lett.* **2022**, *47*, 3660−3663.

(24) Miranda, M.; Fordell, T.; Arnold, C.; L'Huillier, A.; Crespo, H. Simultaneous compression and characterization of ultrashort laser pulses using chirped mirrors and glass wedges. *Opt. Express* **2012**, *20*, 688−697.

(25) Escoto, E.; Tajalli, A.; Nagy, T.; Steinmeyer, G. Advanced phase retrieval for dispersion scan: a comparative study. *JOSA B* **2018**, *35*, 8−19.

(26) Kleinert, S.; Tajalli, A.; Nagy, T.; Morgner, U. Rapid phase retrieval of ultrashort pulses from dispersion scan traces using deep neural networks. *Opt. Lett.* **2019**, *44*, 979−982.

(27) Brar, V. W.; Koltonow, A. R.; Huang, J. New discoveries and opportunities from two-dimensional materials. *ACS Photonics* **2017**, *4*, 407−411.

(28) Hendry, E.; Hale, P. J.; Moger, J.; Savchenko, A. K.; Mikhailov, S. A. Coherent Nonlinear Optical Response of Graphene. *Phys. Rev. Lett.* **2010**, *105*, 097401.

(29) Gomes, T.; Canhota, M.; Kulyk, B.; Carvalho, A.; Jarrais, B.; Fernandes, A. J.; Freire, C.; Costa, F.; Crespo, H. Ultrafast laser pulse characterization by THG d-scan using optically enhanced graphene coatings. *arXiv:2206.01676* **2022** DOI: 10.48550/arXiv.2206.01676.

(30) Janisch, C.; Wang, Y.; Ma, D.; Mehta, N.; Elías, A. L.; Perea-López, N.; Terrones, M.; Crespi, V.; Liu, Z. Extraordinary second harmonic generation in tungsten disulfide monolayers. *Sci. Rep.* **2014**, *4*, 5530.

(31) Malard, L. M.; Alencar, T. V.; Barboza, A. P. M.; Mak, K. F.; de Paula, A. M. Observation of intense second harmonic generation from MoS_2 atomic crystals. *Phys. Rev. B* **2013**, *87*, 201401.

(32) Li, D.; Xiong, W.; Jiang, L.; Xiao, Z.; Rabiee Golgir, H.; Wang, M.; Huang, X.; Zhou, Y.; Lin, Z.; Song, J.; Ducharme, S.; Jiang, L.; Silvain, J.-F.; Lu, Y. Multimodal Nonlinear Optical Imaging of MoS_2 and MoS_2-Based van der Waals Heterostructures. *ACS Nano* **2016**, *10*, 3766−3775.

(33) Ribeiro-Soares, J.; Janisch, C.; Liu, Z.; Elias, A. L.; Dresselhaus, M. S.; Terrones, M.; Cançado, L. G.; Jorio, A. Second Harmonic Generation in WSe_2. *2D Materials* **2015**, *2*, 045015.

(34) Cui, Q.; Muniz, R. A.; Sipe, J. E.; Zhao, H. Strong and anisotropic third-harmonic generation in monolayer and multilayer ReS_2. *Phys. Rev. B* **2017**, *95*, 165406.

(35) Hernandez-Rueda, J.; Noordam, M. L.; Komen, I.; Kuipers, L. Nonlinear Optical Response of a WS_2 Monolayer at Room Temperature upon Multicolor Laser Excitation. *ACS Photonics* **2021**, *8*, 550−556.

(36) Busschaert, S.; Reimann, R.; Cavigelli, M.; Khelifa, R.; Jain, A.; Novotny, L. Transition Metal Dichalcogenide Resonators for Second Harmonic Signal Enhancement. *ACS Photonics* **2020**, *7*, 2482−2488.

(37) Bolhuis, M.; Hernandez-Rueda, J.; van Heijst, S. E.; Tinoco Rivas, M.; Kuipers, L.; Conesa-Boj, S. Vertically-oriented MoS_2 nanosheets for nonlinear optical devices. *Nanoscale* **2020**, *12*, 10491−10497.

(38) Janisch, C.; Mehta, N.; Ma, D.; Elías, A. L.; Perea-López, N.; Terrones, M.; Liu, Z. Ultrashort optical pulse characterization using WS_2 monolayers. *Opt. Lett.* **2014**, *39*, 383−385.

(39) Noordam, M. L.; Hernandez-Rueda, J.; Kuipers, L. Simultaneous Characterization of Two Ultrashort Optical Pulses at Different Frequencies Using a WS2Monolayer. *ACS photonics* **2022**, *9*, 1902−1907.

(40) Li, Y.; Chernikov, A.; Zhang, X.; Rigosi, A.; Hill, H. M.; Van Der Zande, A. M.; Chenet, D. A.; Shih, E.-M.; Hone, J.; Heinz, T. F. Measurement of the optical dielectric function of monolayer transition-metal dichalcogenides: MoS_2, $MoSe_2$, WS_2, and WSe_2. *Phys. Rev. B* **2014**, *90*, 205422.

(41) Ermolaev, G. A.; Stebunov, Y. V.; Vyshnevyy, A. A.; Tatarkin, D. E.; Yakubovsky, D. I.; Novikov, S. M.; Baranov, D. G.; Shegai, T.; Nikitin, A. Y.; Arsenin, A. V.; et al. Broadband optical properties of monolayer and bulk MoS_2. *npj 2D Mater. Appl.* **2020**, *4*, 1−6.

(42) You, J.; Bongu, S.; Bao, Q.; Panoiu, N. Nonlinear optical properties and applications of 2D Mater.: theoretical and experimental aspects. *Nanophotonics* **2018**, *8*, 63−97.

(43) Zeng, H.; Liu, G.-B.; Dai, J.; Yan, Y.; Zhu, B.; He, R.; Xie, L.; Xu, S.; Chen, X.; Yao, W.; et al. Optical signature of symmetry

variations and spin-valley coupling in atomically thin tungsten dichalcogenides. *Sci. Rep.* **2013**, *3*, 1608.

(44) Gong, S.-H.; Alpeggiani, F.; Sciacca, B.; Garnett, E. C.; Kuipers, L. Nanoscale chiral valley-photon interface through optical spin-orbit coupling. *Science* **2018**, *359*, 443−447.

(45) Kesarwani, R.; Simbulan, K. B.; Huang, T.-D.; Chiang, Y.-F.; Yeh, N.-C.; Lan, Y.-W.; Lu, T.-H. Control of trion-to-exciton conversion in monolayer WS_2 by orbital angular momentum of light. *Sci. Adv.* **2022**, *8*, eabm0100.

(46) Sytcevich, I.; Guo, C.; Mikaelsson, S.; Vogelsang, J.; Viotti, A.-L.; Alonso, B.; Romero, R.; Guerreiro, P. T.; Sola, Í. J.; L'Huillier, A.; et al. Characterizing ultrashort laser pulses with second harmonic dispersion scans. *JOSA B* **2021**, *38*, 1546−1555.

(47) Weigand, R.; Sánchez-Balmaseda, M.; Afanador-Delgado, S. M.; Salavagione, H. J. Nonlinear thermal and electronic optical properties of graphene in N-methylpyrrolidone at 800nm with femtosecond laser pulses. *J. Appl. Phys.* **2018**, *124*, 033104.

■ NOTE ADDED AFTER ASAP PUBLICATION

This paper was published on June 15, 2023, with wrong content attached as Supporting Information. The correct version was posted on June 16, 2023.